Printed ISSN 1330–0016
Online ISSN 1333–9133
CD ISSN 1333–8390
CODEN FIZBE7

BARYON RESONANCES IN ELECTROMAGNETIC MESON PRODUCTION

VOLKER D. BURKERT

Jefferson Lab, 12000 Jefferson Avenue, 12000 Newport News, VA 26000, U. S. A.
E-mail address: burkert@jlab.org

Received 17 February 2011; Revised manuscript received 2 October 2011
Accepted 23 November 2011 Online 9 February 2012

An overview is given of the exploration of baryon properties in meson photo- and electroproduction at Jefferson Lab. These processes provide ample information relevant to the study of electromagnetic couplings of baryon resonances and to the search for states, yet to be discovered. The CLAS detector, combined with the use of energy-tagged polarized photons and polarized electrons, as well as polarized targets, and the measurement of recoil polarization, provide the tool for a comprehensive nucleon resonance program. The status of this program, prospects for the coming years and plans for the Jefferson Lab 12 GeV upgrade are described.

PACS numbers: 1.55Fv, 13.60Le, 13.40Gp, 14.20Gk UDC 539.126
Keywords: baryon resonances, photoproduction, transition form factors, polarization

1. Introduction

Nucleons are the stuff of which our world is made. As such they must be at the center of any discussion of why the world we actually experience has the character it does. These words were spoken by Nathan Isgur, champion of meson and baryon spectroscopy, during his last appearance at a scientific conference in 2000 [1]. More than 10 years later, these words serve as a reminder that much is still to be understood about the fundamental building blocks of the world we live in.

Understanding the systematics of the nucleon excitation spectrum is key to understanding the effective degrees of freedom underlying baryonic matter. The most comprehensive predictions of the resonance excitation spectrum come from the various implementations of the constituent quark model based on (broken) SU(6) symmetry [2]. Yet, this model does not include gluonic degrees of freedom that may also be excited, and resonances may be generated dynamically through baryon-meson interactions [3]. Recent developments in Lattice QCD led to predic-

tions of the nucleon spectrum in QCD with dynamical quarks [4], albeit with still large pion masses of 420 MeV. In parallel, the development of dynamical coupled-channel models is being advanced with new vigor. The EBAC group at JLab has demonstrated [5] that coupled-channel effects result in a large shift of the Roper resonance pole mass to 1365 MeV downward from its bare core mass of 1736 MeV, explaining the low physical mass of the state, and resolving the longstanding puzzle of the incorrect mass ordering of $P_{11}(1440)$ and $S_{11}(1535)$ resonances in the constituent quark model.

The various resonance models not only predict different excitation spectra but also the Q^2 dependence of the resonance transition form factors. Mapping out these form factors in meson electroproduction experiments tells us a great deal about the effective degrees of freedom underlying baryon structure and the dependences on the distance scale at which resonances are probed in experiment. Consequently, the JLab baryon resonance program has two main components, the exploration of the baryon spectrum and resonance properties, and the measurement of resonance transition form factors in a large range of Q^2.

2. *Exploring the nucleon spectrum*

It has long been realized that the analysis of differential cross sections in the photoproduction of single pseudoscalar mesons alone results in ambiguous solutions for the contributing resonant partial waves. The N^* program at JLab aims at complete, or nearly complete measurements for processes such as $\vec{\gamma}\vec{p} \to \pi N,\ \eta p,\ K\bar{Y}$ and $\vec{\gamma}\vec{n} \to \pi N,\ K^0\vec{\Lambda}$. These reactions are fully described by four complex parity-conserving amplitudes, which may be determined from eight well-chosen combinations of unpolarized cross sections, and single and double-polarization polarization observables using beam, target and recoil polarization measurements. If all combinations are measured, 16 observables can be extracted providing highly redundant information for the determination of production amplitudes [7]. The CLAS detector [6] provides particle identification and momentum analysis in a polar angle range from 8° to 140°. The photon energy tagger provides energy-marked photons with an energy resolution of $\sigma(E)/E = 10^{-3}$. Circularly polarized photons are generated by scattering the highly polarized electron beam from an amorphous radiator. Other equipment includes a coherent bremsstrahlung facility with a precision goniometer for diamond crystal positioning and angle control. The facility has been used for coherent photon bremsstrahlung production, generating photons with linear polarization of up to 90%. There are two frozen-spin polarized targets, one based on butanol as target material (FROST), and one using frozen HD as target material (HDIce). FROST has been operated successfully in two major beam runs. The second production run of 5 months duration has been completed in August 2010.

The HDIce target is currently being assembled. In comparison with FROST, it has a much better dilution factor and figure-of-merit. In the upcoming experiment, it will serve mostly as polarized neutron target although is also provides polarized protons. The experiment [8] is scheduled to take data in 2011 and 2012.

A major focus of the CLAS program is on the hyperon channels, where high-statistics cross-section and polarization data have been measured [9 – 15]. The advantage of hyperon channels is that the weak decay $\Lambda \to p\pi^-$ is self analyzing, allowing to measure the Λ recoil polarization in CLAS. In conjunction with the polarized beam and targets, this enables measurement of all 15 polarization observables that are accessible in the reaction $\gamma p \to K^+\Lambda$. Figure 1 shows high statistics samples of cross section in 10 MeV bins covering a range of 250 MeV in invariant mass. Figure 2 shows the Λ recoil polarization in the same invariant mass range as the cross section. The precision of that data set is also very high. We see that the differential cross section exhibits a rather monotonic behavior and peaks at forward angles, while the recoil polarization shows stronger variation in polar angle, which is indicative of underlying interference effects that could result from resonance behavior that only a complex analysis of many measured observables can reveal. The curves represent a coupled-channel fit of the Bonn-Gatchina (BnGa) group that also includes several hadronic channels.

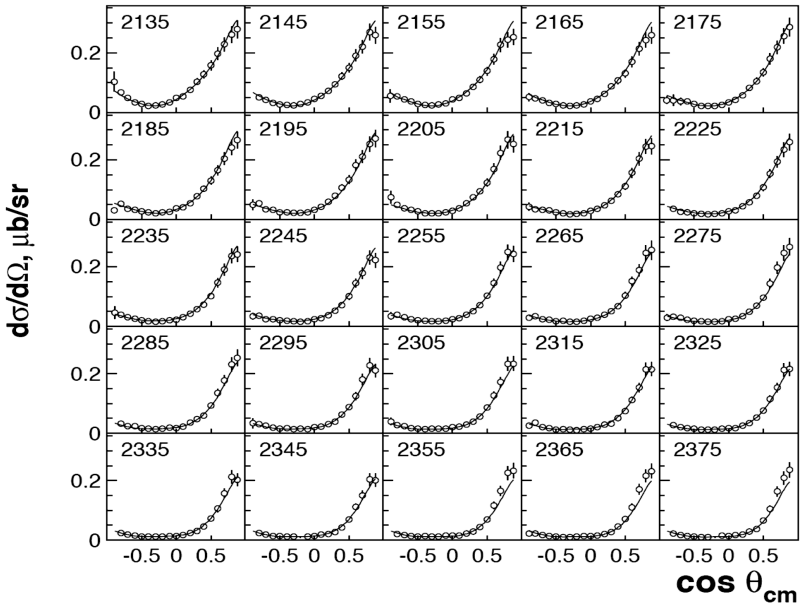

Fig. 1. Polar-angle dependence of the $\gamma p \to K^+\Lambda$ differential cross section for $-1 < \cos\theta^* < 1$.

The total integrated cross section is shown in Fig. 3. The curves are the result of the BnGa fit [16] to the recently published CLAS data [12]. The observed resonant structure in the $J^P = 3/2^+$ partial wave represents the strongest evidence to date for the presence of the quark model state $P_{13}(1900)$. This state is predicted in the symmetric constituent quark model, and provides evidence against the diquark-quark model with point-like di-quark as constituents. This model has no room for such a state in that mass range [17].

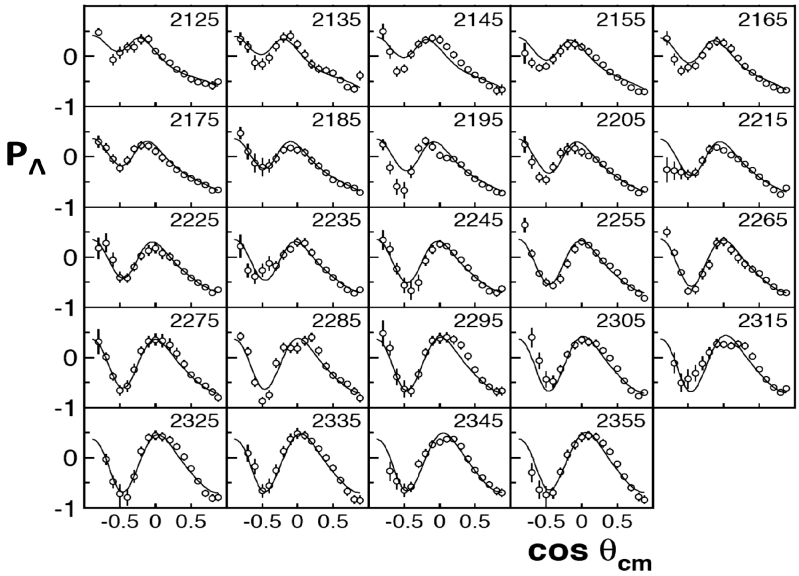

Fig. 2. Angular dependence of the Λ *recoil polarization* P_Λ *in the range* $-1 < \cos\theta^* < 1$.

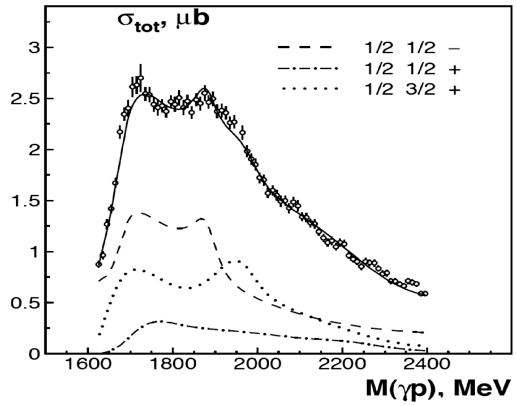

Fig. 3. Total cross section of $\gamma p \to K^+\Lambda$. *The solid curve represents the results of the Bonn-Gatchina analysis of the CLAS data. The analysis requires the* $P_{13}(1900)$, *a state predicted in the symmetric constituent quark model, that has not been confirmed experimentally.*

In channels with nucleons in the final state, where the recoil polarization is usually not measured, seven independent observables are obtained directly. The recoil polarization, which is not measured directly in this experiment, can be inferred from a beam-target double-polarization measurement. High statistics measurements of differential cross section for π^0, π^+, π^-, η, η' and ω have been completed [18 – 20], while analyses of polarization observables for these reactions are in still progress.

For $p\omega$ production, the $\omega \to \pi^+\pi^-\pi^0$ decay distribution contains information on the ω polarization and provides additional constraints in the partial wave analysis. In CLAS, the final state is fully determined by measuring the charged pions, and inferring the π^0 through the overdetermined kinematics as the incident photon energy is measured event-by-event in the photon energy tagging spectrometer. The fit to the phase motion of the dominant partial waves is shown in Fig. 4. It requires the inclusion of three well known resonances, $F_{15}(1680)$, $D_{13}(1700)$, $G_{17}(2190)$), as well as the quark model state $F_{15}(2000)$, an unconfirmed 2^* state in RPP [21]. The need to include the $G_{17}(2190)$ into the fit is the first evidence that this state couples to $p\omega$.

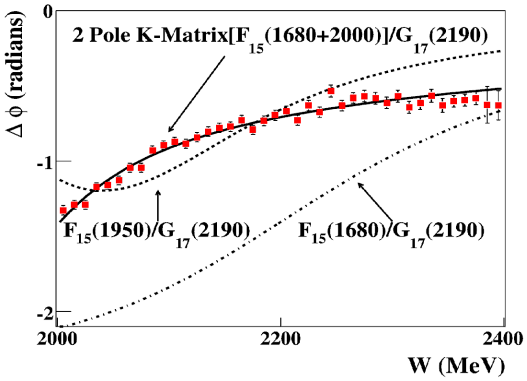

Fig. 4. Fit results for $\Delta\phi = \phi_{7/2^-} - \phi_{5/2^+}$ vs. the invariant $p\omega$ mass. The dot-dashed line is the phase motion expected using constant width Breit-Wigner distributions and the parameters quoted by the PDG for the $F_{15}(1680)$ and $G_{17}(2190)$. The dashed line required the $J^P = 7/2^-$ parameters to be within the PDG limits for the $G_{17}(2190)$, while allowing the $J^P = 5/2^+$ parameters to vary freely. The solid line fit used a constant-width Breit-Wigner distribution for the $G_{17}(2190)$, and a 2-pole single-channel K-matrix for the $J^P = 5/2^+$ wave.

3. *Electromagnetic transition form factors of nucleon resonances*

Electromagnetic transition form factors encode information about the transition charge and magnetization densities [22], which in turn reflect the electromagnetic structure of the excited states. The non-relativistic constituent quark model (nr-CQM) provides a reasonable representation of the mass spectrum of many excited states below 2 GeV. Relativized versions, e.g. in Ref. [17], give qualitative agreement with some of the measured transition amplitudes. Notable exceptions are the $\Delta(1232)$ transition, and the $P_{11}(1440)$, or "Roper" resonance. The magnitude of the $\Delta(1232)$ transition is significantly underestimated in the constituent quark model (CQM), and the Roper amplitudes have a Q^2 dependence that is qualitatively very different from what the model predicts. The nrCQM represent this state as radial

excitation of the nucleon. It has diffculties to describe its basic features such as the mass, photocouplings, Q^2 evolution. In fact, the photocoupling amplitude has the wrong sign, and its magnitude is predicted to rise strongly at small Q^2, contrary to the data that show a rapid drop.

Recently published analysis by the CLAS collaboration included new high statistics $n\pi^+$ data [30] that covered the mass region from pion threshold to 1.7 GeV/c^2. In addition, large samples of differential cross section data [26, 31, 32] and polarization observables [33] taken earlier with CLAS in the channels $p\pi^0$ and $n\pi^+$ are included in a comprehensive analysis of nearly 120,000 data points covering a large range in θ_π, ϕ_π, W and Q^2. Also, cross section data from the $p\eta$ final state [34, 35] were used to independently determine amplitudes of the transition to the $N(1535)S_{11}$ state. This allows one to constrain the branching ratio $\beta_{N\pi}$ and $\beta_{N\eta}$ for this state more accurately.

Two independent approaches, fixed-t dispersion relations and the unitary isobar model, have been employed to estimate the model-sensitivity of the resulting transition amplitudes [36, 37] for the three low-mass states, $N(1440)P_{11}$, $N(1520)D_{13}$ and $N(1535)S_{11}$. The results for these low-mass states that can shed new light on the nature of these states are reviewed in the following sections.

3.1. The $\Delta(1232)$ *resonance*

An interesting aspect of nucleon structure at low energies is a possible quadrupole deformation of the lowest excited state, the $\Delta(1232)$. Such a deformation is evident in finite values of the quadrupole transition amplitudes E_{1+} and S_{1+}, which otherwise would be equal to zero [38]. Quadrupole ratios $R_{EM} = E_{1+}/M_{1+}$ and $R_{SM} = S_{1+}/M_{1+}$ are shown in Fig. 5. The development of sophisticated phenomenological analysis methods over the past decade [39 – 41] resulted in a

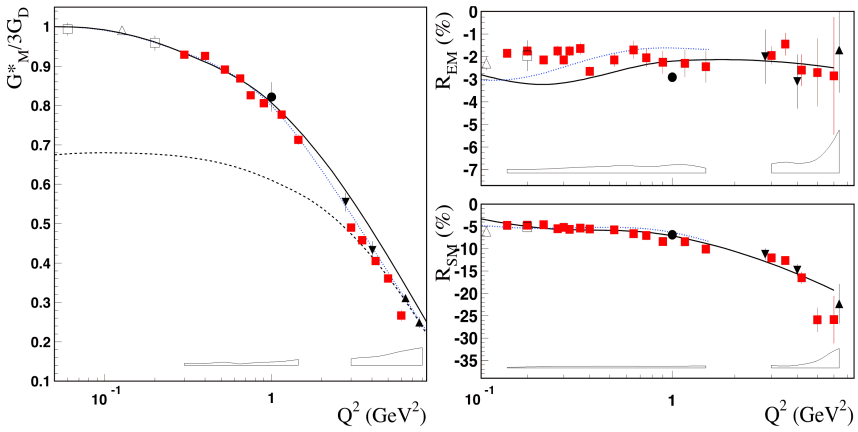

Fig. 5. Left panel: The $\Delta(1232)$ *magnetic transition form factor. Right panel: Quadrupole ratios* R_{EM} *and* R_{SM} *from* $p\pi^0$ *electroproduction,* $p(e,e'p)\pi^0$*. Data from Refs. [23 – 29].*

consistent picture for these quantities. R_{EM} remains negative, small and nearly constant in the entire range $0 < Q^2 < 6$ GeV^2 covered with data. There are no indications that leading pQCD contributions are important, which would require $R_{EM} \to +1$ [42]. The longitudinal quadrupole ratio R_{SM} also remains negative, but its magnitude rises strongly with increasing Q^2. Simultaneous description of both R_{EM} and R_{SM} is achieved with dynamical models that include pion-nucleon interactions explicitly, supporting the idea that most of the quadrupole strength in the $N\Delta(1232)$ transition is due to meson effect [43, 44].

3.2. The Roper resonance $P_{11}(1440)$

The difficulties in describing the $P_{11}(1440)$ resonance in constituent quark models has prompted the development of alternative models involving gluon fields [45], meson-baryon degrees of freedom [46, 47] and quark model description on the light-cone [48, 49]. In particular, measurements of its transition amplitudes in pion electroproduction have revealed information about the nature of the state.

Given these different theoretical concepts for the structure of the state, the question "what is the nature of the Roper state?" has been a focus of the N^* program with CLAS. The state is wide, and pion electroproduction data covering a large range in the invariant mass W with full center-of-mass angular coverage are key in extracting the transition form factors. As an isospin $I = 1/2$ state, the $P_{11}(1440)$ couples more strongly to $n\pi^+$ than to $p\pi^0$. Also, contributions of the high energy tail of the $\Delta(1232)$ are much reduced in that channel due to the $I = 3/2$ nature of the $\Delta(1232)$. Previous studies [40] have mostly used the $p\pi^0$ final state from measurements focusing on the $\Delta(1232)$ mass region.

The results of the most recent analysis of the transverse and longitudinal amplitudes $A_{1/2}$ and $S_{1/2}$ of the $P_{11}(1440)$ resonance are shown in Fig. 6. At the

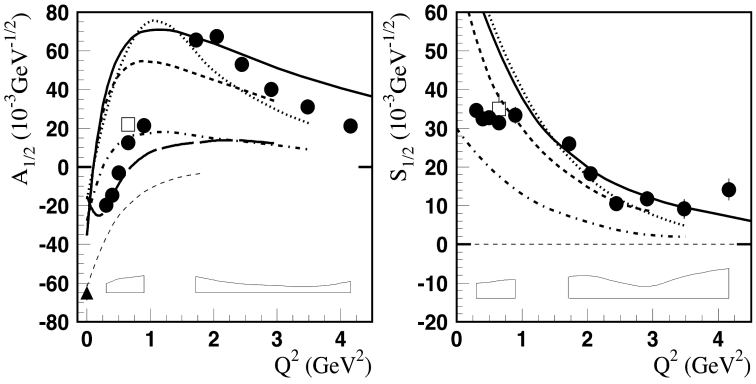

Fig. 6. Transverse electrocoupling amplitude for the Roper $P_{11}(1440)$ (left panel). The full circles are the new CLAS results. The squares are previously published results of fits to CLAS data at low Q^2. The right panel shows the longitudinal amplitude. The bold curves are all relativistic light-front quark model calculations [49]. The thin dashed line is for a gluonic excitation [45].

real photon point, $A_{1/2}$ is negative, rises quickly with Q^2, and changes sign near $Q^2 = 0.5$ GeV^2. At $Q^2 = 2$ GeV^2, the amplitude reaches the same magnitude but with opposite sign as at $Q^2 = 0$ before it slowly falls off with Q^2. This remarkable sign change with Q^2 has not been observed before for any nucleon form factor or transition amplitude. In fact, the Roper, which is a relatively small resonance at the real photon point, becomes a prominent excited state at high Q^2, where both amplitudes are qualitatively described by the light front quark models. The interpretation of the state as a radial excitation of the nucleon is therefore consistent with its behavior at short distances. The low Q^2 (large distance) behavior is not well described by the LF quark models which fall short of describing the amplitude at the photon point. This suggests that important contributions, e.g. meson-baryon interactions describing the large distances behavior, are missing, as has also been recently demonstrated in a covariant valence quark model [50, 51]. A first exploration of the Roper transition form factors has recently been undertaken within lattice QCD [52].

3.3. The $S_{11}(1535)$ resonance

This state has been studied extensively in the $p\eta$ channel, where it appears as an isolated resonance near the $N\eta$ threshold. Phenomenological analyses of data from CLAS [53, 54] and Hall C [55, 56] have resulted in the Q^2 evolution of the transverse transition amplitude $A_{1/2}$ from η electroproduction data. However, there are two remaining uncertainties that need to be examined. One of them is due to the branching ratio of the coupling $S_{11}(1535) \to p\eta$. The PDG [21] gives ranges of $\beta_{N\eta}^{PDG} = 0.45 - 0.60$ and $\beta_{N\pi}^{PDG} = 0.35 - 0.55$, which adds a large uncertainty to the resulting helicity amplitudes. Since this state has very small coupling to channels other than $N\eta$ and $N\pi$, a measurement of the reaction $ep \to e\pi^+ n$ can reduce this uncertainty. In the CLAS analysis [37], we obtain $\beta_{N\pi} = 0.485 \pm 0.008 \pm 0.023$ and $\beta_{N\eta} = 0.46 \pm 0.008 \pm 0.022$, which brings the two data sets into excellent agreement, as shown in Fig. 7. Another uncertainty comes from the lack of precise information

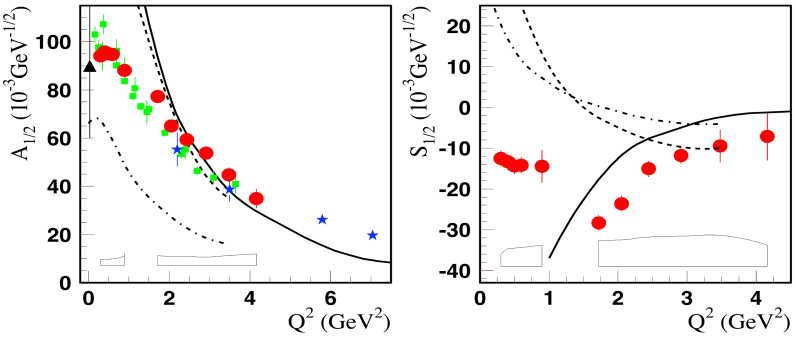

Fig. 7. The transition amplitude $A_{1/2}$ (left) for the $S_{11}(1535)$. The full circles are from the analysis of the CLAS $n\pi^+$ and $p\pi^0$ data [61, 62]. The other data are from the analysis of $p\eta$ data [53–56]. The curves represent constituent quark model calculations [48, 63, 64].

on the longitudinal coupling. This contribution is usually assumed to be equal to zero when analyzing the $p\eta$ channel, which will affect the extraction of $A_{1/2}$. An important advantage of the $N\pi$ channel is that it is also sensitive to the longitudinal transition amplitude $S_{1/2}$ resulting from strong $s-p$ wave interference with the p-wave amplitude of the nearby $P_{11}(1440)$. Since the $P_{11}(1440)$ does not couple to $p\eta$, this channel has very little sensitivity to the $S_{1/2}$ amplitude for this transition.

3.4. Helicity structure of the $D_{13}(1520)$

A longstanding prediction [65] of the dynamical constituent quark model is the helicity switch from the dominance of the $A_{3/2}$ amplitude at the photon point to $A_{1/2}$ dominance at $Q^2 > 1$ GeV^2. Indications of such behavior have been observed in previous analysis [39, 40], but analyses have been hampered by incomplete kinematical coverage of data, and the scarceness of $n\pi^+$ data, which are most sensitive to the excitation of the state. The new CLAS data have largely eliminated this shortcoming. Figure 8 shows the CLAS results for the electrocouplings. The $A_{3/2}$ amplitude is large and dominating at the real photon point, but decreases rapidly in strength with increasing Q^2. $A_{1/2}$ is small at the photon point and increases rapidly in magnitude with increasing Q^2. At high Q^2, $A_{1/2}$ becomes the dominant amplitude, which confirms the early prediction of the constituent quark model.

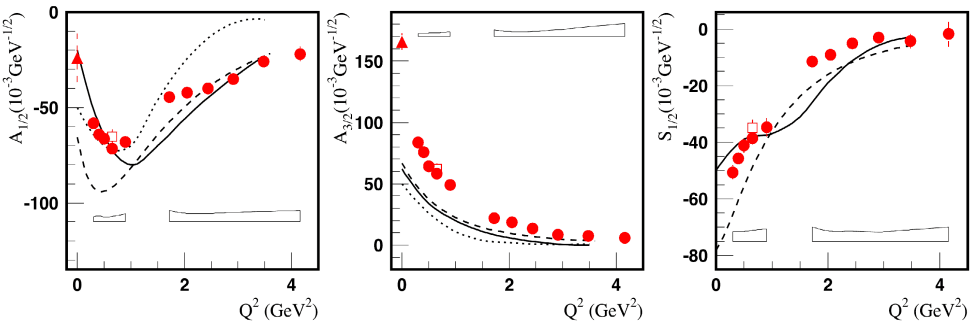

Fig. 8. Electrocoupling amplitudes $A_{1/2}$ (left), $A_{3/2}$ (middle) and $S_{1/2}$ (right) for the $D_{13}(1520)$. Model curves as in Fig. 7.

4. Two-pion electroproduction

Single-pion production is particularly sensitive to the lower-mass spectrum as low-mass states dominantly couple to the $N\pi$ final state. Many of the higher-mass states, e.g. $\Delta(1620)$, $\Delta(1700)$, $N(1720)$, and $\Delta(1970)$, couple with probabilities up to 90% to $N\pi\pi$ final states. Electroproduction of two pions in the final state thus provides another opportunity to study exited baryon states and determine their transition form factors. The channel $ep \to e'p\pi^+\pi^-$ has large non-resonant

contributions as can be seen in the total cross section displayed in Fig. 9. However, a careful analysis that takes into account all major processes has shown to be sensitive to the resonant terms due to strong interference terms [71]. The $P_{11}(1440)$ transition amplitudes were extracted from the $p\pi^+\pi^-$ data at small Q^2. They are in very good agreement with analysis of the $N\pi$ final state despite the much different background contributions for the two processes. In the range above 1.7 GeV, the 2-pion channel can be more sensitive to resonances than other channels, making it an effective tool in the search for new states and the extraction of transition form factors of high-mass states.

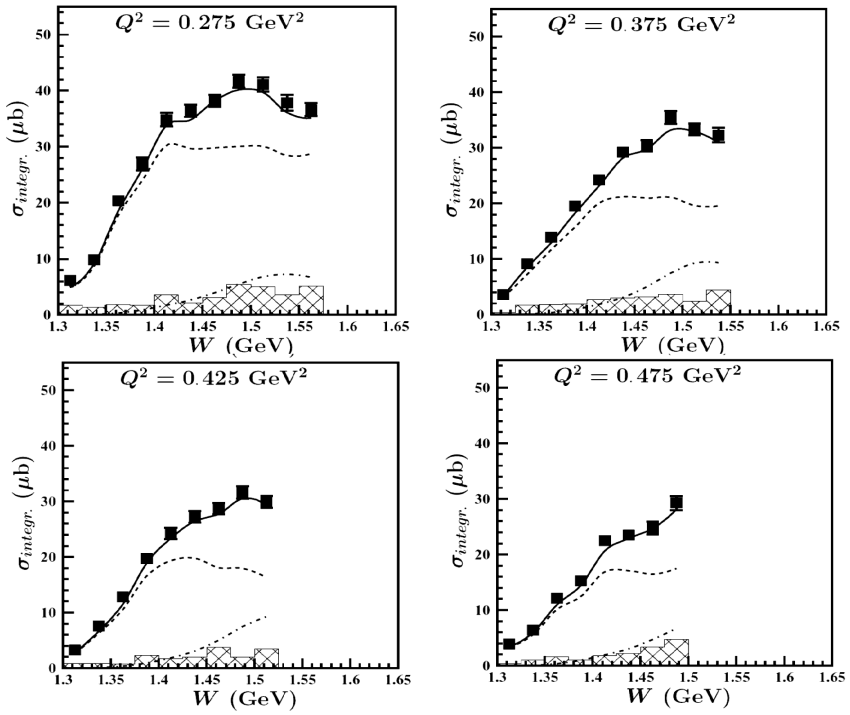

Fig. 9. Total cross section for $\gamma^* p \to p\pi^+\pi^-$ at different Q^2 values.

5. *Strangeness electroproduction*

In theoretical studies [68], it was found that kaon electroproduction should have strong sensitivity to the excitation of nucleon resonances. Cross section measurements of strangeness channel, e.g. $ep \to eK^+Y^0$, and polarization transfer measurements $\vec{e}p \to eK^+\vec{Y}^0$ ($Y^0 = \Lambda, \Sigma$) have been carried out [66, 67] that allow stringent tests of hadronic models. The separated structure functions in Fig. 10 and Fig. 11 reveal clear differences in the production dynamics for the two channels. The

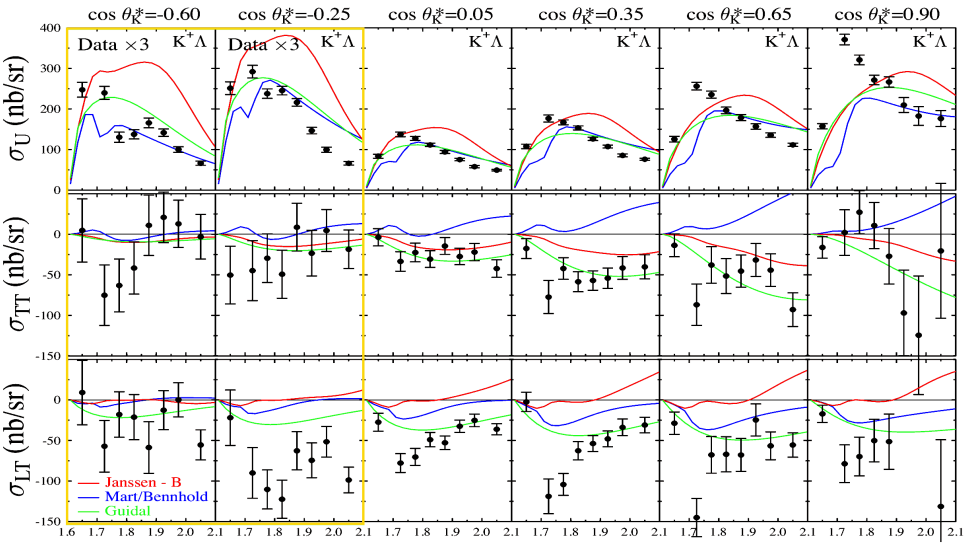

Fig. 10. Separated cross section for the electroproduction of the $K^+\Lambda$ and final state.

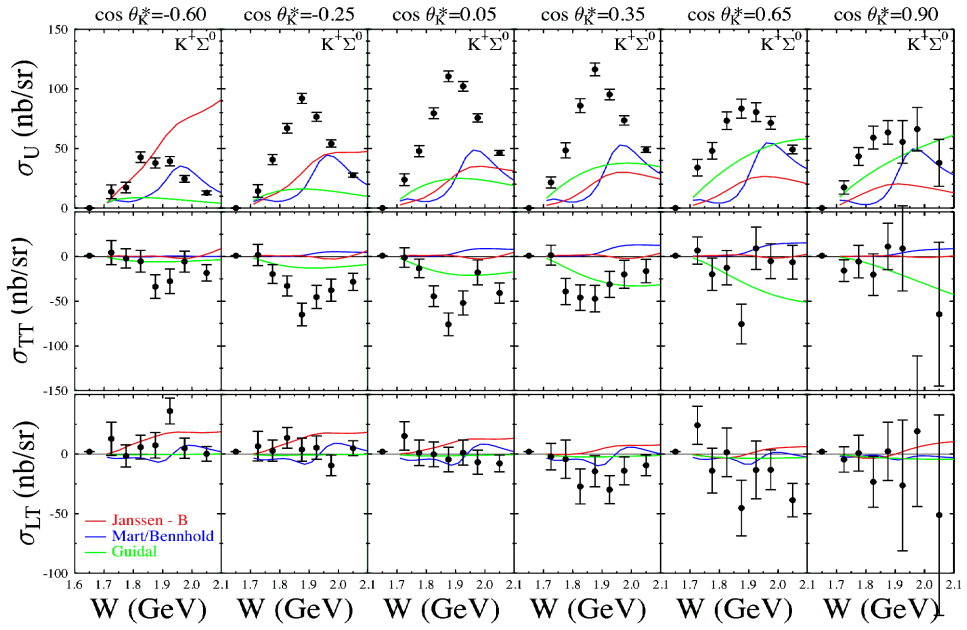

Fig. 11. Separated cross section for the electroproduction of the $K^+\Sigma$ final state.

ϕ-independent response function $\sigma_U = \sigma_T + \epsilon\sigma_L$ for the $K^+\Lambda$ channel quickly rises above threshold and drops off smoothly at higher mass. This behavior is qualitatively reproduced in hadron models that incorporate resonance just above threshold that may have a signicant $K^+\Lambda$ coupling, such as $P_{11}(1710)$ and $P_{13}(1720)$. The σ_{LT} response function is an interference of transverse and longitudinal amplitudes. It is large and indicates the presence of strong longitudinal couplings. This behavior is quite different from the one for the $K^+\Sigma^0$ channel where the σ_{LT} response is small, even compatible with zero, while the σ_{TT} interference response is sizable. Note that the response function σ_L was not separated in these measurements and the strength of the longitudinal amplitude can only be inferred from the interference term. The σ_U response for $K^+\Sigma^0$ shows indications of strong s-channel strength near 1.9 GeV. Hadronic models that include known resonances are not able to describe the large resonance-like structure leaving ample room for additional resonances to possibly contribute. These data provide important constraints for dynamically coupled-channel analyses.

6. Conclusion and outlook

A large effort is currently underway at Jefferson Lab to probe the $S = 0$ baryon excitation spectrum in photoproduction measurements of varies baryon-meson final states. These include cross sections and multiple polarization observables, both with polarized beam and polarized targets, as well as recoil polarization measurements. Measurement on proton targets have been completed in an extended run with transversely polarized proton target in 2010. The program on the neutron is planned to be completed with a photon run using polarized HD material in 2011/2012. This will complete the 6 GeV era N^* program to search for excited states of the nucleon that have not been observed before.

The determination of transition amplitudes from electroproduction data for many high-mass states is ongoing. Precise transition amplitudes have been published for the low-mass resonances. The $p\pi^+\pi^-$ final state is being analyzed to study both low-mass states [69] and higher-mass states that dominantly couple to $N\pi\pi$ channels such as $S_{31}(1620)$, $D_{33}(1700)$ and $P_{11}(1720)$ [70, 71]. A new experiment [72] in Hall A is in preparation to study the $\Delta(1232)$ resonance at very small Q^2 where pion cloud contributions are expected to be large and the R_{EM} and R_{SM} ratios that are sensitive to such contributions are not known. The experiment is scheduled to run in the spring of 2011. Lastly, a program to measure resonance transition form factors at photon virtuality $5 < Q^2 < 12$ GeV^2 has been approved for the CLAS12 detector [73, 74]. CLAS12 is currently under construction as part of the JLab 12 GeV upgrade project and is expected to be fully operational in 2015.

Acknowledgements

I like to thank members of the CLAS collaboration for producing much of the data presented in this paper. This work was performed under DOE contract DE-AC05-060R23177.

References

[1] N. Isgur, *Why N*s are important*, in *Excited Nucleons and Hadronic Structure*, Proc. NSTAR 2000 Conf., ed. V. D. Burkert et al., World Scientifc (2001); e-Print: nucl-th/0007008.

[2] N. Isgur and G. Karl, Phys. Rev. D **18** (1978) 4187; Phys. Rev. D **19** (1979) 2653.

[3] E. Oset et al., Int. J. Mod. Phys. A **20** (2005) 1619.

[4] J. M. Bulava et al., Phys. Rev. D **79** (2009) 034505.

[5] H. Kamano, S. X. Nakamura, T.-S. H. Lee and T. Sato, Phys. Rev. C **81** (2010) 065207.

[6] B. Mecking et al., Nucl. Instrum. Meth. A **503** (2003) 513.

[7] A. Sandorfi, S. Hoblit, H. Kamano and T.-S. H. Lee, arXiv:1010.4555 [nucl-th].

[8] A. Sandorfi, F. J. Klein et al., JLab experiment E06-101 (2006).

[9] J. W. McNabb et al., Phys. Rev. C **69** (2004) 042201.

[10] R. Bradford et al., Phys. Rev. C **73** (2006) 035202; Phys. Rev. C **75** (2007) 035205.

[11] I. Hleiqawi et al., Phys. Rev. C **75** (2007) 042201; Erratum, ibid. **76** (2007) 039905.

[12] M. McCracken et al., Phys. Rev. C **81** (2010) 025201.

[13] S. Anafalos Pereira et al., Phys. Lett. B **688** (2010) 289.

[14] B. Dey et al., Phys. Rev. C **82** (2010) 025202.

[15] L. Guo et al., Phys. Rev. C **76** (2007) 025208.

[16] A.V. Anisovich et al., arXiv:1009.4803, (2010), [hep-ph].

[17] M. Aiello, M. M. Giannini and E. Santopinto, J. Phys. G **24** (1998) 753.

[18] M. Dugger et al., Phys. Rev. Lett. **89** (2002) 222002; Phys. Rev. Lett. **96** (2006) 062001; Phys. Rev. C **76** (2007) 025211; Phys. Rev. C **79** (2009) 065205.

[19] W. Chen et al., Phys. Rev. Lett. **103** (2009) 012301.

[20] M. Williams et al., Phys. Rev. C **80** (2009) 065208; Phys. Rev. C **80** (2009) 065209; Phys. Rev. C **80** (2009) 045213.

[21] K. Nakamura et al. (Particle Data Group), JPG **37** (2010) 075021.

[22] L. Tiator and M. Vanderhaeghen, Phys. Lett. B **672** (2009) 344.

[23] S. Stave et al., Phys. Rev. C **78** (2008) 025209; N. F. Sparveris et al., Phys. Lett. B **561** (2007) 102.

[24] N. F. Sparveris et al., Phys. Rev. Lett. **94** (2005) 022003.

[25] V. V. Frolov et al., Phys. Rev. Lett.**82** (1999) 45.

[26] K. Joo, et al, Phys. Rev. Lett. **88** (2002) 122001; Phys. Rev. C **68** (2003) 032201; Phys. Rev. C **70** (2004) 042201; Phys. Rev. C **72** (2005) 058202.

[27] M. Ungaro et al., Phys. Rev. Lett. **97** (2006) 112003.

[28] J. J. Kelly et al., Phys. Rev. Lett. **95** (2005) 102001.

[29] A. N. Villano et al., Phys. Rev. C **80** (2009) 035203.

[30] K. Park et al., Phys. Rev. C **77** (2008) 015208.

[31] H. Egiyan et al., Phys. Rev. C **73** (2006) 025204.

[32] M. Ungaro et al., Phys. Rev. Lett. **97** (2006) 112003.

[33] A. Biselli et al., Phys. Rev. C **68** (2003) 035202; Phys. Rev. C **78** (2008) 045204.

[34] R. Thompson et al., Phys. Rev. Lett. **86** (2001) 1702.

[35] H. Denizli et al., Phys. Rev. C **76** (2007) 015204.

[36] I. Aznauryan et al., Phys. Rev. C **78** (2008) 045209.

[37] I. Aznauryan et al., Phys. Rev. C **80** (2009) 055203.

[38] A. Buchmann and E. Henley, Phys. Rev. D **65** (2002) 073017.

[39] For recent reviews see: V. D. Burkert and T.-S. H. Lee, Int. J. Phys. E **13** (2004) 1035; I. G. Aznauryan and V. D. Burkert, Prog. Part. Nucl. Phys. **67** (2012) 1.

[40] D. Drechsel, et al., Eur. Phys. J. A **34** (2007) 69.

[41] I. Aznauryan, Phys. Rev. C **67** (2003) 015209.

[42] G. A. Warren and C. E. Carlson, Phys. Rev. D **42** (1990) 3020.

[43] T. Sato and T. S. Lee, Phys. Rev. C **63** (2001) 055201.

[44] S. S. Kamalov and S. N. Yang, Phys. Rev. Lett. **83** (1999) 4494.

[45] Z. P. Li, V. D. Burkert and Zh. Li, Phys. Rev. D **46** (1992) 70.

[46] F. Cano and P. Gonzales, Phys. Lett. B **431** (1998) 270.

[47] O. Krehl et al., Phys. Rev. C **62** (2000) 025207.

[48] S. Capstick and B. D. Keister, Phys. Rev. D **51** (1995) 3598.

[49] For an overview, see: I. Aznauryan, Phys. Rev. C **76** (2007) 025212.

[50] G. Ramalho and K. Tsushima, Phys. Rev. D **81** (2010) 074020.

[51] G. Ramalho, F. Gross, M. T. Pena and K. Tsushima, arXiv:1008.0371 [hep-ph].

[52] H.-W. Lin et al., Phys. Rev. D **78** (2008) 114508.

[53] R. Thompson et al., Phys. Rev. Lett. **86** (2001) 1702.

[54] H. Denizli, Phys. Rev. C **76** (2007) 015204.

[55] C. S. Armstrong et al., Phys. Rev. D **60** (1999) 052004.

[56] M. M. Dalton et al., arXiv:0804.3509 [hep-ex].

[57] H. Egiyan at al., Phys. Rev. C **73** (2006) 025204.

[58] K. Joo et al., Phys. Rev. C **70** (2004) 042201.

[59] K. Joo et al., Phys. Rev. C **72** (2005) 058202.

[60] A. Biselli et al., Phys. Rev. C **78** (2008) 045204.

[61] I. Aznauryan et al., Phys. Rev. C **71** (2005) 015201; Phys. Rev. C **72** (2005) 045201.

[62] I. Aznauryan et al. (CLAS), Phys. Rev. C **78** (2008) 045209.

[63] E. Pace, G. Salmé and S. Simula, Few Body Syst. Suppl. **10** (1999) 407.

[64] V. M. Braun, et al., arXiv:0902.3087 (hep-ph).
[65] F. E. Close and F. J. Gilman, Phys. Lett. B **38** (1972) 541.
[66] P. Ambrozewicz et al., Phys. Rev. C **75** (2007) 045203.
[67] D. Carman et al., Phys. Rev. Lett. **90** (2003) 131804; Phys. Rev. C **79** (2009) 065205.
[68] R. A. Williams et al., Phys. Rev. C **46** (1992) 1617.
[69] G. V. Fedotov et al., Phys. Rev. C **79** (2009) 015204.
[70] M. Ripani et al., Phys. Rev. Lett. **91** (2003) 022002.
[71] V. Mokeev et al., Phys. Rev. C **80** (2009) 045212.
[72] N. Sparveris et al., JLab experiment E08-010.
[73] R. Gothe, V. Mokeev et al., JLab experiment E12-09-003.
[74] V. D. Burkert, arXiv:0810.4718 [hep-ph].

BARIONSKE REZONANCIJE U ELEKTROMAGNETSKOJ TVORBI MEZONA

Daje se pregled istraživanja svojstava bariona u mezonskoj foto- i elektrotvorbi u Jeffersonovom Laboratoriju. Ti procesi pružaju obilne podatke koji se odnose na elektromagnetska vezanja barionskih rezonzncija i na traženje stanja koja još treba otkriti. Detektor CLAS i upotreba polariziranih fotona i elektrona označene energije zajedno s polariziranim metama i mjerenjem odbojne polarizacije su uređaji za iscrpne programe istraživanja nukleonskih rezonancija. Opisuje se napredak tih programa, izgledi za naredne godine i planovi za dogradnju ubrzivača do energije 12 GeV.